

Stellar velocity dispersion in narrow-line Seyfert 1 galaxies

V. Botte,^{★†} S. Ciroi,[†] F. Di Mille, P. Rafanelli and A. Romano

Department of Astronomy, University of Padova, vicolo dell'Osservatorio 2, I-35122 Padova, Italy

Accepted 2004 October 12. Received 2004 September 13; in original form 2004 June 30

ABSTRACT

Several authors have recently explored, for narrow-line Seyfert 1 galaxies (NLS1s), the relationship between black hole mass (M_{BH}) and stellar velocity dispersion (σ_*). Their results are more or less in agreement and seem to indicate that NLS1s fill the region below the fit obtained by Tremaine et al., showing a range of σ_* similar to that of Seyfert 1 galaxies, and a lower M_{BH} . Until now, the [O III] width has been used in place of the stellar velocity dispersion, but some indications have begun to arise against the effectiveness of the gaseous kinematics in representing the bulge potential, at least in NLS1s. Bian & Zhao have stressed the urgency of producing true σ_* measurements. Here, we present new stellar velocity dispersions obtained through direct measurements of the Ca II absorption triplet ($\sim 8550 \text{ \AA}$) in the nuclei of eight NLS1 galaxies. The resulting σ_* values and a comparison with $\sigma_{[\text{O III}]}$ confirm our suspicion that [O III] typically overestimates the stellar velocity dispersion. We demonstrate that NLS1s follow the $M_{\text{BH}}-\sigma_*$ relation as Seyfert 1, quasars and non-active galaxies.

Key words: galaxies: active – galaxies: kinematics and dynamics – galaxies: nuclei – galaxies: Seyfert.

1 INTRODUCTION

Recently, there has been great interest in the study of the correlation between the mass of nuclear supermassive black holes (BHs), M_{BH} , and the stellar velocity dispersion, σ_* , of their hosting bulges. This relation has been obtained for nearby non-active galaxies by several authors (Gebhardt et al. 2000a; Ferrarese & Merritt 2000; Tremaine et al. 2002; Marconi & Hunt 2003), supporting the theory that the growth of the BH is bound to galaxy formation. According to Di Matteo et al. (2003), this correlation – not set in primordial structures but fully established only at low redshift – can be understood if there is a simple linear relation between the total gas mass in galaxies and their M_{BH} .

In their sample Gebhardt et al. (2000b) included seven active galactic nuclei (AGNs) and found that these objects also followed a similar $M_{\text{BH}}-\sigma_*$ correlation of non-active galaxies. Other authors then confirmed the validity of this result for samples of Seyfert 1 galaxies (S1s) and quasars (Nelson 2000; Ferrarese et al. 2001; Wandel 2002; Boroson 2003; Shields et al. 2003). However, no consensus has been reached until now about the case of narrow-line Seyfert 1 galaxies (NLS1s). These AGNs have spectroscopic properties slightly different from those of classical S1s, e.g. narrower permitted emission lines in the optical wavelength domain and steeper power-law X-ray continua, which suggest that NLS1s are hosting BHs with smaller masses accreting at high rates, close to

the Eddington limit. This hypothesis would imply that NLS1s have also less massive bulges than classical S1s, of course assuming that their M_{BH} are correlated to the physical properties of their hosting bulges. Indeed, Wang & Lu (2001) and Wandel (2002, 2004) found that there is no clear difference in the $M_{\text{BH}}-\sigma_*$ relation between narrow-line and broad-line AGNs and non-active nearby galaxies; however, opposite results were obtained by Mathur, Kuraszewicz & Czerny (2001), Bian & Zhao (2004a), Grupe & Mathur (2004) and Botte et al. (2004). The main problem is that σ_* in AGNs is available for few S1s and only three NLS1s: Mrk 110 ($90 \pm 7 \text{ km s}^{-1}$) by Ferrarese et al. (2001), NGC 4051 ($88 \pm 13 \text{ km s}^{-1}$) by Nelson & Whittle (1995) and Mrk 766 ($106 \pm 40 \text{ km s}^{-1}$) by Jiménez-Benito et al. (2000). In place of σ_* , the [O III] emission linewidth was extensively used as a representation of the bulge velocity dispersion.

Here we present new direct determinations of σ_* in the nuclei of eight NLS1 galaxies, obtained using the Ca II absorption triplet (8498, 8542, 8662 \AA). The targets were extracted from Botte et al. (2004), except for Mrk 766. In Section 2 we present the spectroscopic observations and the data reduction. In Section 3 we give a detailed description of the methods we used to measure stellar and gaseous kinematics, and we present the results. Finally, in Section 4 we discuss the implications of our results on the validity of the $\text{FWHM}([\text{O III}])/2.35 = \sigma_*$ and $M_{\text{BH}}-\sigma_*$ relations for NLS1 galaxies.

2 OBSERVATIONS AND DATA REDUCTION

We have observed the nuclei of seven NLS1s with the Asiago Faint Object Spectrograph Camera (AFOSC) mounted at the 1.82-m

[★]Guest investigator of the UK Astronomy Data Centre.

[†]E-mail: botte@pd.astro.it (VB); ciroi@pd.astro.it (SC)

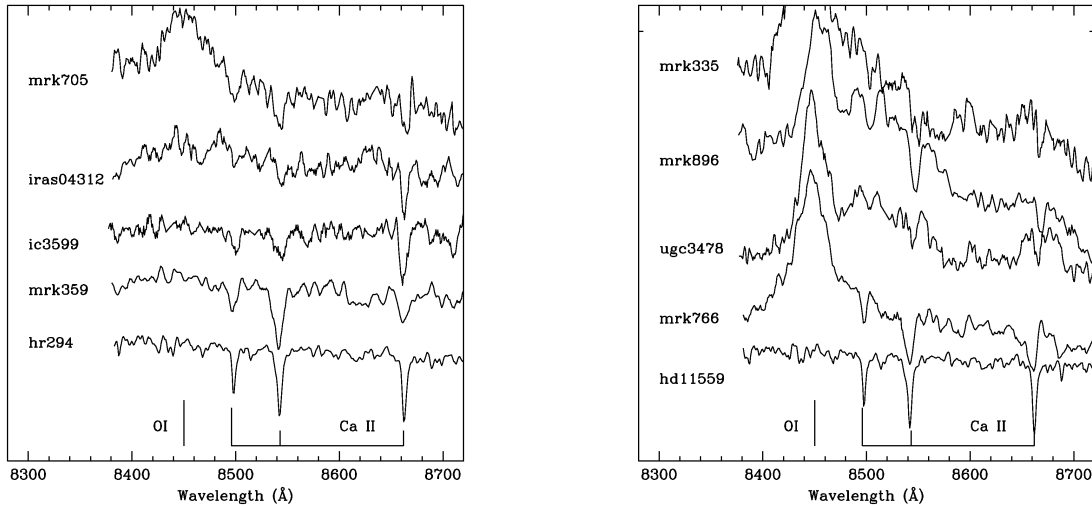


Figure 1. The rest-frame spectra of the eight NLS1s showing the Ca II triplet absorption lines. The template stars (HR 294 and HD 11559) are also plotted for comparison.

telescope of the Padova Astronomical Observatory (Asiago, Italy). A volume phase holographic grism (Bianco et al. 2003) was used in combination with a 1.69-arcsec slit to cover the region $\sim 8200\text{--}9200$ Å which includes the Ca II triplet absorption lines, with a dispersion of ~ 0.88 Å px^{-1} and a relatively high spectral resolution (~ 50 km s^{-1}). Mrk 766 was also observed in the optical wavelength range (4300–8000 Å) at medium resolution, in order to derive the M_{BH} and [O III] width information not available in Botte et al. (2004) and useful for the following analysis. In addition to galaxy observations, the spectra of two template stars, HR 294 (G9 III) and HD 11559 (K0 III), were obtained for kinematic analysis with the same configuration. Two spectral types were chosen to minimize the template mismatch effects.

Mrk 896 was extracted from the Isaac Newton Group (ING) Archive. A spectrum covering a larger range ($\sim 7700\text{--}9400$ Å) was obtained in 1994 August at the William Herschel Telescope (Canary Islands, Spain) with the ISIS Double Beam Spectrograph. The R316R grating used in combination with a 1.47-arcsec slit yielded a dispersion of ~ 1.35 Å px^{-1} and an instrumental resolution of ~ 65 km s^{-1} . A standard star (BD+17 4708) was observed during the same run for spectrophotometric calibration.

The spectra are shown in Fig. 1. Details about the observations are given in Table 1.

All data were reduced with the same procedure. The usual reduction steps, i.e. bias and flat-field corrections, cosmic ray removal, wavelength calibration by means of comparison lamps and sky-background subtraction, were carried out with IRAF packages.¹ The optical spectrum of Mrk 766 was also flux calibrated through the observation of two spectrophotometric standard stars, FEIGES6 and G191-B2B.

For each object we extracted the nuclear spectrum summing a number of pixels along the slit to increase the signal-to-noise (S/N) ratio. An aperture of ~ 3.3 arcsec (7 pixel) was chosen for the Asiago data on the basis of the seeing, which ranged between 2 and 3 arcsec during the observations. This aperture corresponds to $\sim 0.6\text{--}2$

¹ IRAF is written and supported by the National Optical Astronomy Observatories (Tucson, Arizona), which are operated by the Association of Universities for Research in Astronomy, Inc., under cooperative agreement with the National Science Foundation.

Table 1. Observation log.

Galaxy	z	$\Delta\lambda$ (Å)	Date	T_{exp} (s)
Mrk 359	0.017	8200–9200	2003-09-08	7200
Mrk 335	0.026	8200–9200	2003-12-07	9000
UGC 3478	0.013	8200–9200	2003-12-08	7200
Mrk 705	0.029	8200–9200	2003-12-08	7200
IRAS 04312 + 4008	0.020	8200–9200	2004-01-26	7200
IC 3599	0.022	8200–9200	2004-01-26	7200
Mrk 766	0.013	4300–6500	2004-01-29	2400
		6200–8000	2004-01-30	1800
		8200–9200	2004-01-30	7200
Mrk 896	0.026	7700–9500	1994-08-16	1800

kpc for galaxies in the range $0.01 < z < 0.03$. For the ING spectrum, we used an aperture of 1.7 arcsec (5 pixel), corresponding to ~ 0.9 kpc, following similar arguments.

3 DATA ANALYSIS

3.1 Stellar velocity dispersion

To measure σ_* we have used the Fourier cross-correlation method as implemented in the IRAF task FXCOR, which is based on the method of Tonry & Davis (1979). The spectrum of the galaxy G and the stellar template T are resampled into N bins, where each bin number n is proportional to $\ln \lambda$, and cross-correlated in Fourier space:

$$C(n) = G(n) \times T(n) = \int_{-\infty}^{\infty} T(k)G(k+n) dk. \quad (1)$$

Here, \times means cross-correlation.

This method assumes that $G(n)$ is a convolution of $T(n)$, representing the true stellar population in the galaxy, with a broadening function $b(n)$, offset from zero velocity by an amount δ

$$g(n) \propto b(n - \delta) * t(n) = \int_{-\infty}^{\infty} b(x - \delta)t(n - x) dx, \quad (2)$$

where $*$ denotes convolution.

The maximum peak of the cross-correlation function (CCF) is fitted by a smooth symmetric function (in general, a Gaussian function), whose location and width are related to the galaxy redshift and velocity dispersion of the stars in the galaxy. In order to recover σ_* from the FWHM of the CCF peak, we adopted the suggestions given by Nelson & Whittle (1995). We convolved the template spectrum with Gaussian functions of known increasing dispersions (from 10 to 300 km s⁻¹) and we measured the corresponding increasing widths of the CCF peak. Then, we fitted the empirical FWHM– σ_* relationship with a polynomial function.

Before running FXCOR, the spectra of the NLS1s were moved to the rest frame and their continuum carefully removed. This last step proved to be rather important, because the cross-correlation method is sensitive to low-frequency fluctuations and our targets are often characterized by emission lines and/or bumps. In particular, five out of the eight observed targets show the O I λ 8446 emission line, and in at least three galaxies (Mrk 335, Mrk 896, UGC 3478) the Ca II absorptions are overlapped to broader Ca II emissions. Then, FXCOR was run using two template stars for the Asiago data, and the only one available for the ING archival data. The resulting CCF peaks had values of the Tonry–Davis R parameter (Tonry & Davis 1979), a sort of S/N indicator, ranging from 8 to 20. No filtering of high-frequency noise was applied, because we verified that it was not necessary and we introduced variations of the results depending on the arbitrary choice of the filter shape.

To estimate the uncertainty of the σ_* measurements, we followed Ohya et al. (2002). First, two spectral regions were independently correlated for each template spectrum: 8300–8800 and 8450–8750 Å. This allowed us to have four values of σ_* for each galaxy. We adopted the mean of these measurements and calculated the rms ($\delta\sigma_1$). $\delta\sigma_1$ was not estimated for Mrk 896, because only one template star was available. Then, we made 20 spectra for each object by adding artificial noise with the IRAF task MKNOISE to increase the rms by ~ 20 per cent. FXCOR was run again 20 times with these new spectra and the scatter of the peak width measurements was adopted as an error of the CCF peak fitting ($\delta\sigma_2$). Finally, the uncertainty of the instrumental resolution ($\delta\tau \sim 2\text{--}4$ km s⁻¹) was considered as an additional source of error by deriving equation (18) of Tonry & Davis (1979): $\delta\sigma_3 = 2\tau\delta\tau/\sigma_*$. Assuming these errors are independent of each other, the total $\Delta\sigma_*$ was obtained through the following relation:

$$\Delta\sigma_* = \sqrt{(\delta\sigma_1)^2 + (\delta\sigma_2)^2 + (\delta\sigma_3)^2}.$$

The stellar velocity dispersions are listed in Table 2.

3.2 Gas velocity dispersion

In addition to measurements of stellar kinematics from absorption lines, we took from our previous work (Botte et al. 2004) the optical spectra of the same objects, containing the narrow-line region (NLR) emission lines, which allow to measure the gas kinematics. In particular, the width of the [O III] λ 5007 line was measured and then corrected for instrumental line broadening to determine the velocity dispersion of the gas in the NLR. Because the [O III] emission line is bright in these spectra, its profile is very little affected by noise. Therefore, we fitted [O III] with Gaussian functions only changing for five times the continuum level, chosen by visual inspection. The average dispersion $\sigma_{[\text{O III}]}$ and its relative scatter were calculated for each galaxy. The gas velocity dispersions are given in Table 2.

Table 2. Stellar and gaseous velocity dispersions, and BH masses.

Galaxy	σ_* (km s ⁻¹)	$\sigma_{[\text{O III}]}$ (km s ⁻¹)	M_{BH} ($\times 10^6 M_{\odot}$)
Mrk 335	64 \pm 17	140.8 \pm 3.4	8.61
Mrk 359	112 \pm 12	67.0 \pm 0.4	0.69
UGC 3478	89 \pm 18	109.8 \pm 2.6	0.81
Mrk 705	82 \pm 25	185.9 \pm 2.1	46.13
IRAS 4312	64 \pm 20	136.8 \pm 7.8	0.83
IC 3599	85 \pm 17	106.9 \pm 4.4	0.13
Mrk 766	81 \pm 17	131.2 \pm 0.7	0.63
Mrk 896	87 \pm 11	129.6 \pm 0.6	4.43
Mrk 110	90 \pm 7 ^a	123.3 ^b	6.65 ^c
NGC 4051	88 \pm 13 ^d	81 ^b	1.35 ^c

^aAverage value from Ferrarese et al. (2001).

^bFrom Whittle (1992).

^cAverage value from Kaspi et al. (2000).

^dFrom Nelson & Whittle (1995).

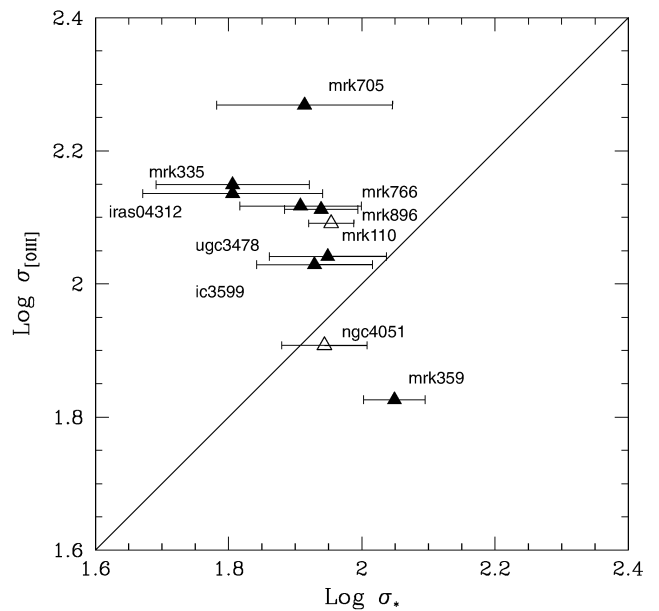


Figure 2. Stellar versus gas kinematics. Solid triangles are the observed galaxies, while open triangles are the two additional NLS1s taken from literature. The solid line is $\sigma_{[\text{O III}]} = \sigma_*$.

3.3 Results

Fig. 2 shows σ_* values versus [O III] widths ($\sigma_{[\text{O III}]}$). The result is very interesting because it clearly shows that [O III] systematically overestimate the stellar velocity dispersion in NLS1s. In fact, all targets except one (Mrk 359) occupy the upper half of the σ_* – $\sigma_{[\text{O III}]}$ plane, and are not grouped around the 1:1 separation line. In other words, this is the first indication that using $\sigma_{[\text{O III}]}$ in place of σ_* could be wrong in NLS1s, which seem to have $\langle\sigma_*\rangle \sim 84 \pm 14$ km s⁻¹. In this picture, Mrk 359 is an outlier. It is the only case among our data having $\sigma_{[\text{O III}]} < \sigma_*$. A justification was given by Jiménez-Benito et al. (2000), who suggested that such cases could be caused by gas settled in a cold rotating disc.

Fig. 3 shows the new σ_* data plotted versus the BH masses. M_{BH} values (Table 2) are taken from Botte et al. (2004) except for

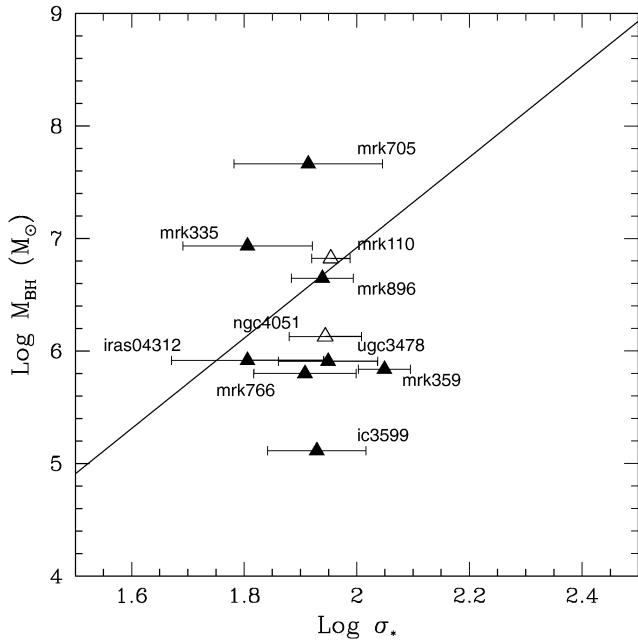


Figure 3. Stellar velocity dispersion versus BH mass. The solid line is the Tremaine et al. (2002) fit. Symbols are the same as in Fig. 2.

Mrk 766, which was observed also in the optical range between 4000 and 6000 Å to measure the FWHM(H β) and the continuum luminosity at rest frame $\lambda = 5100$ Å as well as the [O III] width. Its $\sigma_{[\text{O III}]}$ and BH mass value are also listed in Table 2. In both figures, open triangles indicate Mrk 110 and NGC 4051, two additional NLS1s with known σ_* , mentioned in Section 1. Their $\sigma_{[\text{O III}]}$ and M_{BH} values are taken from the literature. For Mrk 766, we used our measurements, which are in agreement with Jiménez-Benito et al. (2000) within the error bars.

It is clear from Fig. 3 that these new σ_* values fill a range more in agreement with the Tremaine et al. (2002) relation: $\log M_{\text{BH}} = 4.02 \log \sigma_* - 1.12$, considering a mass range of $\sim 10^6$ – $10^7 M_{\odot}$ for BHs in NLS1s. In fact, after having plotted our data over the $M_{\text{BH}}-\sigma_*$ relation, we see that NLS1s are well arranged around the Tremaine et al. fit, and not systematically below the fit as previously found. The data show a significant scatter around the fit, not very different from that observed in ordinary S1s (see, for example, Wang & Lu 2001; Wandel 2002; Botte et al. 2004). Moreover, five out of 10 NLS1s have a factor of 3–10 lower BH masses than predicted from the $M_{\text{BH}}-\sigma_*$ relation. This would suggest that NLS1s have a tendency to lower M_{BH}/σ_* ratios relative to non-active galaxies and broad-line AGNs, but the limited number of points does not allow us to draw a conclusion about this point.

4 DISCUSSION AND CONCLUSIONS

Several authors have tested the $M_{\text{BH}}-\sigma_*$ correlation validity for AGNs assuming that the gaseous component could reasonably trace the nuclear gravitational potential. In particular, the [O III] width was used as a surrogate of the stellar velocity dispersion, essentially for a practical reason: the [O III] emission line is usually bright in AGNs and therefore easily measurable even in the case of distant objects. In contrast, stellar absorptions require longer integration time and/or large telescopes to reach the S/N ratio necessary to give a reliable estimate of the stellar velocity dispersion. The FWHM([O III]) to σ_* conversion was proposed by Nelson & Whittle (1996), who observed

a large sample of AGNs in two spectral ranges, one including H β , [O III] emission lines and Mg b triplet absorption, and the other containing the Ca II triplet absorption. The data of 66 objects were plotted showing a moderate correlation with a significant scatter. More recently, Jiménez-Benito et al. (2000) obtained similar results on a sample of Seyfert 1 and 2 galaxies, demonstrating that the majority of the galaxies form a cloud of points around the 1 : 1 line of the gas versus stellar velocity dispersion plot, with very weak or even no correlation.

None the less, the use of the [O III] width in place of direct σ_* measurements led Bian & Zhao (2004a), Grupe & Mathur (2004) and Botte et al. (2004) to demonstrate that S1s agree with the $M_{\text{BH}}-\sigma_*$ relation given by Tremaine et al. (2002), even if with a large scatter of σ_* (from 50 to more than 500 km s $^{-1}$), while NLS1 galaxies do not. Moreover, NLS1s appear systematically arranged below the Tremaine et al. fit. Interestingly, this result was already included in Boroson (2003), who carried out an analysis of the $M_{\text{BH}}-[\text{O III}] \lambda 5007$ width relation for 107 low-redshift radio-quiet quasi-stellar objects and S1s. He found that this correlation is real, but the scatter is large, about 0.2 dex. Really, it is easy to verify that the narrow-line AGNs (FWHM(H β) < 2000 km s $^{-1}$) of his sample are mostly located below the Tremaine et al. fit. Therefore, authors were induced to believe that NLS1s do not follow the BH–bulge correlation as S1s, quasars and normal galaxies. However, very recently, Bian & Zhao (2004b) obtained a good consistency in BH mass estimates of NLS1s by using H β and soft X-ray luminosity, while no agreement was found with the [O III] linewidth. Their result casts doubt on the reliability of [O III] as an indicator of stellar velocity dispersion, at least for NLS1s. Indeed, it should be mentioned that the FWHM([O III])/2.35 = σ_* relation was obtained by Nelson & Whittle (1996) for a sample of Seyfert 1 and 2 galaxies, but it was never verified for NLS1s.

The situation clearly required new direct σ_* measurements. We obtained these values for eight NLS1s observing their Ca II triplet. The choice of this spectral range was induced by the fact that NLS1s are very often characterized by large Fe II emission multiplets (4400–4700 and 5150–5350 Å) in correspondence with the absorption lines commonly used to estimate σ_* , such as Mg I $\lambda 5175$ and Fe I $\lambda 5269$. Unfortunately, as shown by Persson (1988), NLS1s with strong Fe II are likely to have Ca II in emission rather than in absorption.

By comparing stellar and gaseous kinematics we found that the FWHM([O III])/2.35 = σ_* relation does not seem to hold for NLS1s, which are arranged mostly at values of $\sigma_{[\text{O III}]}$ larger than expected. Contrary to the recent findings, the direct σ_* measurements span a narrower range typically lower than 100 km s $^{-1}$, and such a range is in agreement with the stellar velocity dispersions expected by the $M_{\text{BH}}-\sigma_*$ relation given by Tremaine et al. (2002) in the case of $M_{\text{BH}} \sim 10^6$ – $10^7 M_{\odot}$. Indeed, with our σ_* determinations, NLS1s are arranged around this relationship, suggesting that, in NLS1s, BH and bulge correlate, and lower-mass BHs correspond to lower stellar velocity dispersions, or in other words lower-mass bulges. We stress that this result is in agreement with our previous work (Botte et al. 2004), where we showed that NLS1s are mostly confined to the lower ranges of the $M_{\text{BH}}-L_{\text{bulge}}(B)$ plane, and are well correlated to S1s and quasars. The fact that the stellar velocity dispersion in place of the gaseous velocity dispersion yields a tighter relation when correlated with BH mass, is essentially caused by the star kinematics, which is more representative of the bulge gravitational potential than the gas in AGNs. Even if the gas motion is mainly controlled by the mass of the bulge, several observations in the past have shown that the base of the line profiles emitted by the NLR in many active galaxies is hardly reproduced simply assuming

a pure virial motion in the potential of the host galaxy (Veilleux 1991, and references therein). Other important factors or processes can be involved, and these additional processes can be at the origin of the larger scatter observed when FWHM([O III]) is used as a surrogate of σ_* . The interaction between the gas and the ejected radio plasma observed in many Seyfert galaxies may strongly influence the gas kinematics and contribute with outflowing motions of the NLR clouds (Nelson & Whittle 1996). Moreover, supersonic winds generated by the active nucleus are believed to accelerate the smaller clouds of the NLR located closer to the central engine and sometimes dominate their virial velocity (Smith 1993). This effect could be more important in NLS1s, because strong nuclear winds are expected in the case of high accretion rates (Leighly & Halpern 2000). In addition, it was pointed out by Nelson & Whittle (1996) that a slight tendency exists for barred and/or disturbed active galaxies to have broader [O III] emission lines. In conclusion, we have obtained results with important implications, which strongly encourage additional observations to enlarge the sample of the observed galaxies.

ACKNOWLEDGMENTS

This work is based on observations collected at Asiago observatory. We are very grateful to the referee for comments which improved the quality of the paper. This research was partially based on data from the ING Archive.

REFERENCES

- Bian W., Zhao Y., 2004a, MNRAS, 347, 607
 Bian W., Zhao Y., 2004b, MNRAS, 352, 823
 Bianco A., Molinari E., Conconi P., Crimi G., Giro E., Pernechele C., Zerbi F. M., 2003, SPIE, 4842, 22
 Boroson T. A., 2003, ApJ, 585, 647
 Botte V., Ciroi S., Rafanelli P., Di Mille F., 2004, AJ, 127, 3168
 Di Matteo T., Croft R. A. C., Springel V., Hernquist L., 2003, ApJ, 593, 56
 Ferrarese L., Merritt D., 2000, ApJ, 539, L9
 Ferrarese L., Pogge R. W., Peterson B. M., Merritt D., Wandel A., Joseph C. L., 2001, ApJ, 555, L79
 Gebhardt K. et al., 2000a, ApJ, 539, L13
 Gebhardt K. et al., 2000b, ApJ, 543, L5
 Grupe D., Mathur S., 2004, ApJ, 606, L41
 Jiménez-Benito L., Díaz A. I., Terlevich R., Terlevich E., 2000, MNRAS, 317, 907
 Kaspi S., Smith P. S., Netzer H., Mao D., Jannuzi B. T., Giveon U., 2000, ApJ, 533, 631
 Leighly K., Halpern J., 2000, Bull. Am. Astron. Soc., 32, 1195
 Marconi A., Hunt L. K., 2003, ApJ, 589, L21
 Mathur S., Kuraskiewicz J., Czerny B., 2001, NewA, 6, 321
 Nelson C. H., 2000, ApJ, 544, L91
 Nelson C. H., Whittle M., 1995, ApJS, 99, 67
 Nelson C. H., Whittle M., 1996, ApJ, 465, 96
 Ohya Y. et al., 2002, AJ, 123, 2903
 Persson S. E., 1988, ApJ, 330, 751
 Shields G. A., Gebhardt K., Salviander S., Wills B. J., Xie B., Brotherton M. S., Yuan J., Dietrich M., 2003, ApJ, 583, 124
 Smith S. J., 1993, ApJ, 411, 570
 Tonry J., Davis M., 1979, AJ, 84, 1511
 Tremaine S. et al., 2002, ApJ, 574, 740
 Veilleux S., 1991, ApJ, 369, 331
 Wandel A., 2002, ApJ, 565, 762
 Wandel A., 2004, Proc. IAU Symp. 222, Black Holes, Stars and ISM in Galactic Nuclei. Kluwer, Dordrecht, in press (astro-ph/0407399)
 Wang T., Lu Y., 2001, A&A, 377, 52
 Whittle M., 1992, ApJS, 79, 49

This paper has been typeset from a $\text{\TeX}/\text{\LaTeX}$ file prepared by the author.